Radiocarbon, Vol 61, Nr 2, 2019, p 375–393 DOI:10.1017/RDC.2018.147
© 2019 by the Arizona Board of Regents on behalf of the University of Arizona

SELECTING THE MOST RELIABLE ^{14}C DATING MATERIAL INSIDE MORTARS: THE ORIGIN OF THE PADUA CATHEDRAL

Anna Addis[1,2*] • Michele Secco[2,3] • Fabio Marzaioli[4] • Gilberto Artioli[1,2] • Alexandra Chavarría Arnau[5] • Isabella Passariello[6] • Filippo Terrasi[4,6] • Gian Pietro Brogiolo[5]

[1]Dipartimento di Geoscienze, Università di Padova, Italy.
[2]Centro Interdipartimentale di Ricerca per lo Studio dei Materiali Cementizi e dei Leganti Idraulici (CIRCe), Università di Padova, Italy.
[3]Dipartimento di Ingegneria Civile, Edile ed Ambientale, Università di Padova, Italy.
[4]Dipartimento di Matematica e Fisica, Università degli studi della Campania Luigi Vanvitelli, Caserta, Italy.
[5]Dipartimento dei Beni Culturali, Università di Padova, Italy.
[6]Laboratorio CIRCE e INNOVA, Caserta, Italy.

ABSTRACT. In order to radiocarbon (^{14}C) date a building, several components of the mortar could be used, such as the mortar binder, the lime lumps, the charcoal particles and shell fragments eventually present among the aggregates. In particular, the mortar binder requires a purification treatment in order to separate it from other sources of carbon, which could change the ^{14}C signature of the binder invalidating the dating process. Here, we present the application of the Cryo2Sonic method to ^{14}C dating of the ancient building structures unearthed during excavation at the Padua Cathedral complex. The dated samples were pretreated by using Cryo2Sonic method and the improved Cryo2Sonic version 2.0, recently developed by introducing additional steps such as centrifugation of the mortar suspension and gravimetric sedimentation of the binder fractions. The Cryo2Sonic version 2.0 relies heavily on the characterization of the mortar and of the purified binder fractions, allowing the isolation of a reliable ^{14}C datable mortar fraction. Through this new method, the ^{14}C dating of different ancient structures excavated next to the Padua Cathedral allow to identify the first religious complex of the city of Padua (3rd–4th centuries AD).

KEYWORDS: ^{14}C mortar dating, Cryo2Sonic, Cryo2Sonic version 2.0, Padua Cathedral, radiocarbon mortar reliability.

ARCHAEOLOGICAL SETTING

The archaeological excavations (campaigns 2011–2012) carried out next to the Romanesque baptistery of the Cathedral in the city of Padua brought to light a complex stratigraphic sequence related to the late Roman and Medieval evolution of a central part of the Medieval urban area (Chavarría 2017). It is of interest due to the scarcity of published archaeological information available for the early Medieval evolution of this Northern Italian city. This study is of decisive importance for the history of Medieval Padua, in the context of the intense debate in recent decades about the location of the first cathedral of the city and credibility of Paulus Diaconus' account in the *Historia Langobardorum* regarding the destruction of the city by king Agilulf (601 AD) and the flight of its bishop to the coastal lagoon (specifically to Malamocco).

The excavation revealed a series of distinct construction phases, which are briefly summarized. Period I: A Roman period testified by remains of a Roman wall. Period II: Construction of a late Roman building (Building II, Figure 1) with at least 3 visible rooms paved with black and white mosaics, its chronology was archaeologically attributed to the period 4th–7th centuries AD. Period III: At the beginning of the 7th century AD, consistent traces of fire on the mosaic floors as well as carbon and pieces of carbonized wood, testify to the destruction of the building and its demolition (Period IIIa). From the layers covering the Period III floors, besides a large quantity of ceramic shards and glass objects, a substantial amount of marble fragments were recovered related to liturgical furnishings (including a piece of altar table) and stylistically dated to an older period (5th–6th century AD). The presence of a large number of pieces of tegulae and wood indicates that the roof collapsed at that time. The analysis of the materials recovered in this layer dated the destruction at the beginning of the 7th century (Chavarría 2017), in

*Corresponding author. Email: anna.addis@unipd.it.

https://doi.org/10.1017/RDC.2018.147 Published online by Cambridge University Press

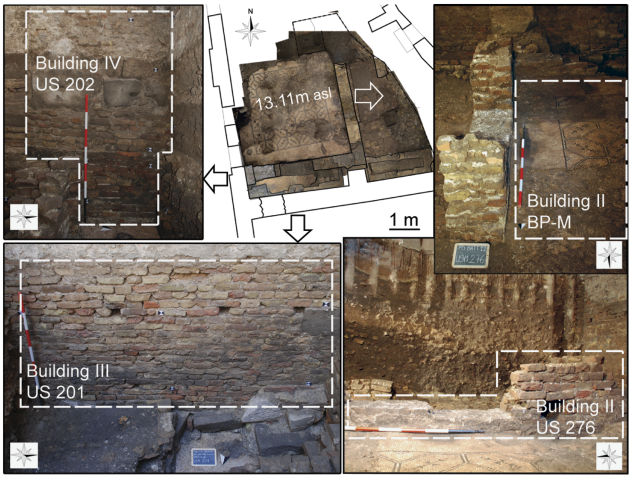

Figure 1 Map and pictures of the archaeological site excavated in the area between the Cathedral Romanesque baptistery and the "Chiostro dei Canonici" in the city of Padua. Sample BP-M: floor bedding mortar of a Roman mosaic from the area of the late Roman building (Building II). Stratigraphic unit US 276: mortar samples 276-36 and 276-41 from the wall surrounding the mosaic. Stratigraphic unit US 201, mortar samples 201-33 and 201-39, from the Building III. Stratigraphic unit US 202: mortar sample 202 from Building IV.

agreement with written sources (Paulus Diaconus, *Historia Langobardorum)* attesting the destruction of the city by the Lombard King Agilulf (601 AD). Period IIIb: The area was later reused for settlement with evidence of postholes and buildings constructed with stones and clay. Four graves (2 infants and 2 adults dated between the 8th and 10th century AD) can be linked to these houses. The area was intensively used, as indicated both by the quick succession of layers and the frequent reconstruction of the buildings. The conclusion of this phase is indicated by a layer of silty soil with varied debris, which obliterated all preceding activity. The construction of a large building (Building III, Figure 1), parallel to the northern wall of the Romanesque baptistery, and of another building linked to it (Building IV, Figure 1), indicates a new and important transformation of the area, which again assumed a Christian liturgical function. These transformations were connected to the construction of a canonical cloister. In this phase, a number of infant burials were placed, in the external area of the early Medieval baptistery (10th–11th century AD; Canci et al. 2017). Finally, a wall was constructed inside the building between the 14th and the 15th century AD, dated through the uses of medieval brick (diffused after the 13th century) and the construction technique.

In summary, the excavations seem to have recovered a section of the late Roman episcopal complex, dated back to the 4th century, probably an area close to the main church or its baptistery, affected by destructions at the beginning of the 7th century when it became to be used as a dump in a marginal area of a settlement, and successively as a poor settlement. The area was not used anymore for public purposes until the end of the Early Middle Ages, when a highly privileged cemetery was established, probably mainly located to the North of the Cathedral baptistery.

Sample Treatments: Cryo2Sonic and Cryo2sonic Version 2.0

In order to radiocarbon (^{14}C) date a building structure such as a wall, several components of the mortar can be employed, such as (1) its binder and lime lumps, which were formed by the

https://doi.org/10.1017/RDC.2018.147 Published online by Cambridge University Press

absorption of atmospheric CO_2 during the carbonation phase, (2) charcoal particles representing a relict of the calcination process, and (3) shell fragments eventually present among the aggregate particles.

The extraction of the fine datable fraction of the binder from the bulk mortar that include a number of unwanted components (especially geological carbonate) is commonly performed by chemical step dissolution methods (Van Strydonck et al. 1983a, 1983b, 1991), physical separation (Nawrocka et al. 2005; Marzaioli et al. 2011, 2013), or mixed physical-chemical technique, based on fractional grain separation together with chemical leaching and gas collection during different time ranges (Soninnen and Jungner 2001; Lindross et al. 2007; Goslar et al. 2009; Nawrocka et al. 2009; Heinemeir et al. 2010; Michalska and Czernik 2015). With the aim of preparing the binder for ^{14}C dating, we used a modification of the *Cryo2Sonic* method based on mechanical fragmentation of the mortar components and separation of the binder from other components (Marzaioli et al. 2011, 2013). The original procedure involved freezing and thawing cycles (Nawrocka et al. 2005; Michalska et al. 2013), followed by a double wet ultra-sonication for 10 and 30 min in order to generate respectively a coarse sand and a fine binder suspension. After sonication, the fractions are isolated by pipetting the upper part of the solutions, which are centrifuged at 20,000 RCF for 5 min and oven-dried overnight (80ºC).

Since 2013 (Nonni et al. 2013), the *Cryo2Sonic* protocol was gradually optimized by adding a mineralogical characterization of the mortars before the entire procedure in order to understand the nature of the sample and to assess the presence of non-binder contamination. Recently, the method has been implemented by modifying some steps of the purification protocol and adding a more extensive characterization of the mortars before and after the purification treatment. At present, the protocol—hereafter called Cryo2sonic version 2.0—consists of four steps (Figure 2):

1. Mortar characterization in order to assess the nature of the contaminants and adopt the correct procedure in order to remove them;
2. Purification treatment by means of sonication, centrifugation and gravimetric sedimentation;
3. Characterization of the obtained powder for the evaluation of the purification treatment effectiveness; and
4. ^{14}C dating of the powder that is composed by pure lime binder devoid of any contaminants. The mortar characterization is based on both petrographic and mineralogical analyses by means of several techniques, such as optical microscopy (OM), cathodoluminescence-induced optical spectroscopy (CL-OS) and x-ray powder diffraction (XRPD). Using the information obtained from mortar characterization, the purification protocol is better defined in terms of number of cycles and duration of each step. The mortar is ultra-sonicated in an ultrasonic bath by using ultra-pure water and centrifuged. Then, it is suspended in ultra-pure water for 20 hr, in order to obtain a dimensional separation of the binder particles that are usually smaller than 5 μm, according to Stokes' law that gives the velocity of a particle with known diameter and density that moves through a fluid at a specific gravity acceleration. At the end of the sedimentation time, the uppermost suspension is sampled and filtered by using a vacuum pump system and inorganic 0.1 μm filters.

After the purification procedure, the powders obtained are checked again using x-ray powder diffraction and cathodoluminescence-induced optical spectroscopy in order to evaluate

https://doi.org/10.1017/RDC.2018.147 Published online by Cambridge University Press

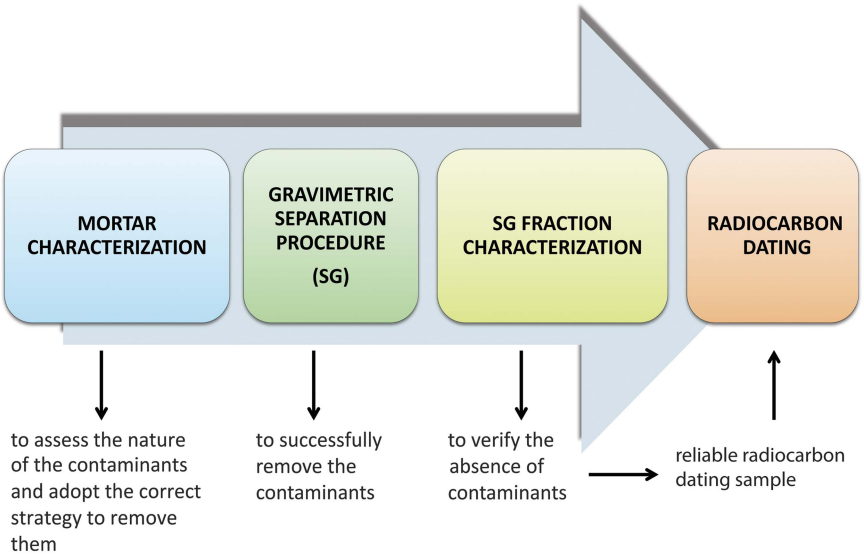

Figure 2 The steps of Cryo2sonic version 2.0 (v.2.0). The protocol consists of four steps: (1) mortar characterization, (2) gravimetric separation treatment, (3) characterization of the obtained powder, and (4) ^{14}C dating of the powder that is composed by pure lime binder devoid of any contaminants.

effectiveness of the purification treatment (i.e. the purity of the binder and the absence of geological carbonates). The ^{14}C dating is exclusively performed on the fractions that are composed of pure lime binder.

METHODS AND MATERIALS

The mortars of three structures unearthed during the excavation at the Padua Cathedral were sampled and selected for the analysis (Figure 1). From the area of the late Roman building (Building II), the floor bedding mortar of a Roman mosaic (sample BP-M), and the mortars of the wall surrounding the mosaic (samples 276-36 and 276-41 of the US 276) were analyzed.

From the structures parallel to the northern wall of the Romanesque baptistery (US 201 of Building III), and of another building linked to it (US 202 of Building IV), mortar samples 201-33, 201-39 and 202 were investigated. The sample analysis was divided into two parts:

1. The mortar characterization, the separation of the binder fraction and its characterization are performed at the CIRCe Center in Padua (Inter-Departmental Research Center for the Study of Cement Materials and Hydraulic Binders); and
2. The graphitization and the AMS measurements are carried out at the CIRCE Center in Caserta (Center for Isotopic Research on the Cultural and Environmental Heritage).

The petrographic analyses were performed by means of a Nikon Eclipse ME600 microscope equipped with a Canon EOS 600D Digital single-lens reflex camera. The cathodoluminescence observations were carried out by using a NIKON Labophot2-POL microscope equipped with a cold cathode stage Cambridge Image Technology Ltd, CL8200 MK3 operated at a voltage of 15 kV and current of 200 μA.

https://doi.org/10.1017/RDC.2018.147 Published online by Cambridge University Press

The quantitative crystal phase analyses (QPA) of the bulk samples were performed by full-profile analysis of x-ray powder diffraction (XRPD) data. Semi-quantitative analyses were then performed on the binder fractions, concentrated and separated from the aggregate through the purification methods. XRPD data were collected using a Bragg–Brentano θ-θ diffractometer (PANalytical X'Pert PRO, Cu Kα or Co Kα radiation, 40 kV and 40 mA) equipped with a real time multiple strip (RTMS) detector (X'Celerator by PANalytical). Diffraction patterns were preliminarly interpreted using the X'Pert HighScore Plus 3.0 software by PANalytical, qualitatively reconstructing mineral profiles of the compounds by comparison with PDF databases from the International Centre for Diffraction Data (ICDD). Then, mineralogical quantitative phase analyses were performed using the full-profile method (Rietveld 1969). Refinements were accomplished with the TOPAS software (v.4.1) by Bruker AXS.

^{14}C dating on binder powders obtained by both the Cryo2Sonic and Cryo2Sonic v.2.0 treatments, shell fragments and carbonate standard samples (i.e., IAEA C1 and C2) (Rozansky et al. 2002) was performed by converting the carbonaceous materials to CO_2 by means of 85% orthophosphoric acid digestion for 2 hr at 80°C. Charcoal fragments were treated by hot hydrochloric acid (HCl, 3%) to eliminate carbonates, followed by a treatment with sodium hydroxide (NaOH, 3.2%) to remove the remaining organic acids. The last step is a final acid attack to remove the adsorbed modern CO_2 during the alkaline attack (AAA protocol). At the end the sample was neutralized, dried and combusted. The CO_2 produced by acid digestion or combustion was cryogenically purified and then reduced to graphite according to the CIRCE sealed tube reaction protocol (Marzaioli et al. 2008) and finally measured for ^{14}C isotopic ratios by AMS (Terrasi et al. 2007, 2008; Passariello et al. 2007). Measured ^{14}C ratios were converted to ^{14}C-calibrated ages according to Stuiver and Polach (1977) and calibrated to absolute ages by means of OxCal 4.2 (Ramsey and Lee 2013) using the IntCal13 (Reimer et al. 2013) calibration curve.

Avoiding Contamination through the Mortar Characterization

The aim of mortar characterization is firstly to recognize the presence of datable materials, such as lime binder, lime lumps, charcoal particles, and shell fragments (Figure 3). Secondly, the presence of contaminants (Figure 4)—i.e. components that could modify the ^{14}C signal of the original lime setting date—is investigated in order to evaluate how to separate them from the datable materials by fine tuning the applied separation procedure.

In particular, the petrographic and mineralogical characterizations were aimed to do the following:

1. Verify the type of binder (hydraulic binder, air lime binder, gypsum binder, earthen binder or mixed types of binders). In fact, the ^{14}C mortar method is only applicable to air lime-based mortars or mixed-binder mortars with high amount of lime binder;
2. Identify the type of lime lumps by means of both optical and cathodoluminescence spectroscopy. Generally, the lime lumps are portions of lime binder not well mixed in the mortars and this is the case of datable mortar materials. However, they could be also formed due to a not adequate slaking of the lime putty or they could be produced due to non-homogeneous temperatures in the kiln (under/over-burnt fragments of limestone); in both cases, they could represent sources of contamination for the binder or other datable lime lumps. In fact, careless preparation of the lime putty, inadequate slaking, and lime overburning could produce poorly reactive lime lumps that harden well after the binder carbonation, thus incorporating younger ^{14}C signal. On the other hand, the presence of under-burnt limestone fragments or mixing with geogenic carbonate during slaking induce an old ^{14}C signal;

https://doi.org/10.1017/RDC.2018.147 Published online by Cambridge University Press

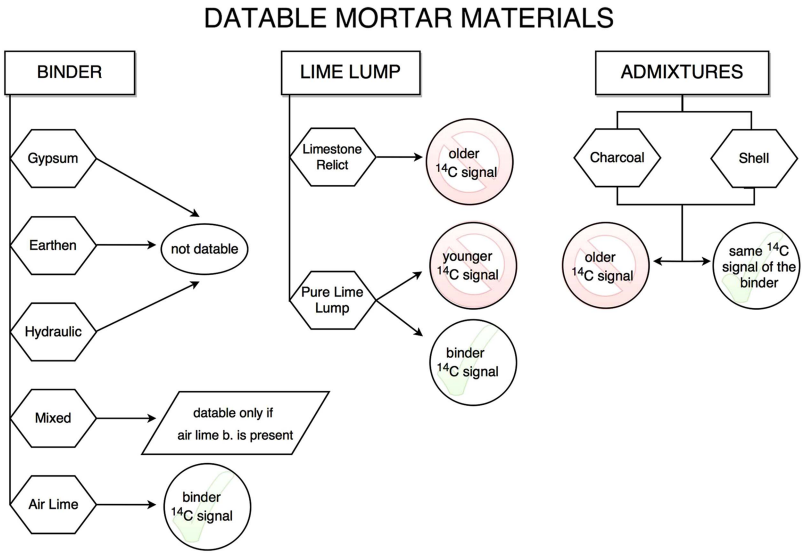

Figure 3 Flow chart of the identification of datable materials within the mortars and their possible contaminations. Types of binder: gypsum – hearten – hydraulic (since no carbonate is present, they are not ^{14}C datable); mixed (datable only if a lime binder is present); and air lime (datable). Types of lime lumps: limestone relict (source of dead carbon that could contaminate the lime binder ^{14}C signal), pure lime lump (depending on the lump setting time, its ^{14}C signals could reflect either the binder setting time or a younger time). Types of admixtures: charcoal and shell (their ^{14}C dating accuracy varies depending if they were contemporary to the time of the wall construction or not).

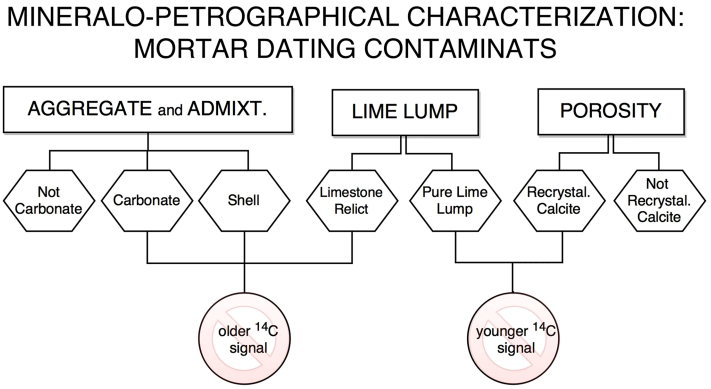

Figure 4 Flow chart of the most common mortar contaminants: carbonate aggregates and limestone relict (source of dead carbon); shell fragments that could have an older ^{14}C signal than the binder, pure lime lump that could harden after the binder; and recrystallized calcite that crystallize after the binder.

3. Regarding the aggregates, the petrographic analysis is aimed at verifying the presence of geologic carbonate aggregate particles, which are extremely dangerous dead carbon bearers. In particular, the estimation of the amount, distribution, and size of the geologic carbonates is essential to eventually separate such components from the binder. Usually, under-burnt fragment of limestone or geogenic carbonates are well identified under the

https://doi.org/10.1017/RDC.2018.147 Published online by Cambridge University Press

cathode-luminescence microscope by the typical red-orange luminescence color of carbonate rocks that is totally absent in the pure binder matrix. In addition, the mineralogical analysis can help to recognize the presence of hydrotalcite—a mineral of the family of double-layered mixed-metal hydroxides (LDH or AFm)—that is a dangerous and poorly known contaminant related to hydraulic lime mortars (Secco et al. 2016). In fact, LDH phases possess exchange capabilities for a variety of organic and inorganic anions including carbon dioxide (Artioli et al. 2017), so that they could modify the original atmospheric CO_2 signal of the mortar. The ^{14}C dating performed on LDH-containing mortars often results in younger age determinations. LDH phases are especially problematic for carbon dating because they frequently accumulate in the fine fraction because of their clay-like nature.

4. The evaluation of the porosity, in which secondary calcite could have been crystallized, is another important point of the mortar characterization. In fact, portions of the binder may be subjected to dissolution and recrystallization processes at later times due to the fluids percolating the masonry unit. The calcite recrystallized at later stages could also affect the dating measurements.
5. The mortar characterization finally allows the identification of any other datable organic and inorganic materials, such as charcoal residues and shell fragments.

RESULTS

Minero-Petrographic Characterization

The mortars of three structures of the Padua Cathedral were analyzed; from Building II the floor bedding mortar (sample BP-M) and two mortars of the surrounding wall (sample 276-36 and 276-41); from Building III two samples were analyzed (201-33 and 201-39), and from Building IV sample 202 was investigated. The samples were collected from the walls and analyzed different times in order to help during the development of the Cryo2sonic optimization.

US 276 and BP-M (Building II)

The petrographic observations (Table 1) of the floor bedding mortar of the Roman mosaic (sample BP-M) and the mortars of the surrounding wall (samples 276-36 in Figure 5a, and 276-41) revealed the presence of air lime binders with a homogenous texture and constituted by calcite crystals with grain size below 5 μm (micritic texture). In the binder matrix, several lime lumps were identified as evidence of the slaking process, during which quick lime was turned into lime putty.

In samples 276-36 and 276-41, the lime lumps observed under a cathodoluminescence microscope are characterized by the typical red luminescence of under-burnt fragments of limestone, which preserve the ^{14}C signal of the rock (Figure 6). The aggregate—with a dimensional range of 0.08–6.40 mm—is composed by polycrystalline quartzite fragments, feldspars and micritic limestones. The presence of carbonate aggregates is confirmed by observations under the cathodoluminescence microscope, in which calcite and dolomite exhibit the typical red luminescence. Sub-spherical pores are present in the samples, likely due to air bubbles entrapped in the mixture. Several fissuring pores were observed in sample 276-41, possibly formed due to shrinkage phenomena. No evidence of calcite recrystallization was observed.

In sample BP-M (Figure 5c), the aggregate size ranges from 0.06 to 2.59 mm, and is mainly composed by monocrystalline quartz crystals, limestones, feldspars, and fragments of ceramics. The mortar is characterized by a well-homogenized lean mixture, in which only few lime lumps

https://doi.org/10.1017/RDC.2018.147 Published online by Cambridge University Press

https://doi.org/10.1017/RDC.2018.147 Published online by Cambridge University Press

Table 1 Characterization of the mortars. B/A: binder to aggregate ratio. Hydr: hydraulic binder, Qz: quartz; lim: limestone; feld: feldspar; CL: presence of luminescence; RoC: risk of contamination; CC re-crystal.: secondary calcite inside the pores.

	Binder			Aggregate					Lime lump			Porosity	
Sample	Type	Texture	B/A	Composition	Min	Max	CL	RoC	Amt.	CL	RoC	CC re-crystal.	RoC
BP-M	Air-lime	Micritic	1/4	Qz, lim, feld, ceramic	0.06	2.59	High	Yes	20%	Weak	Yes	No	No
276-36	Air-lime	Micritic	1/3	Qz, lim, feld	0.09	5.70	High	Yes	10%	High	Yes	No	No
276-41	Air-lime	Micritic	1/3	Qz, lim, feld	0.08	6.30	High	Yes	10%	High	Yes	No	No
201-33	Air-lime; hydr	Micritic	1/2.5	Qz, lim, feld	0.04	0.95	High	Yes	30%	High	Yes	No	No
201-39	Air-lime	Micritic	1/2.5	Qz, lim, feld	0.05	0.90	High	Yes	20%	Null-high	Yes	No	No
202	Air-lime	Micritic	1/4.5	Qz, lim, feld, shell	0.03	1.20	High	Yes	5%	Weak- high	Yes	No	No

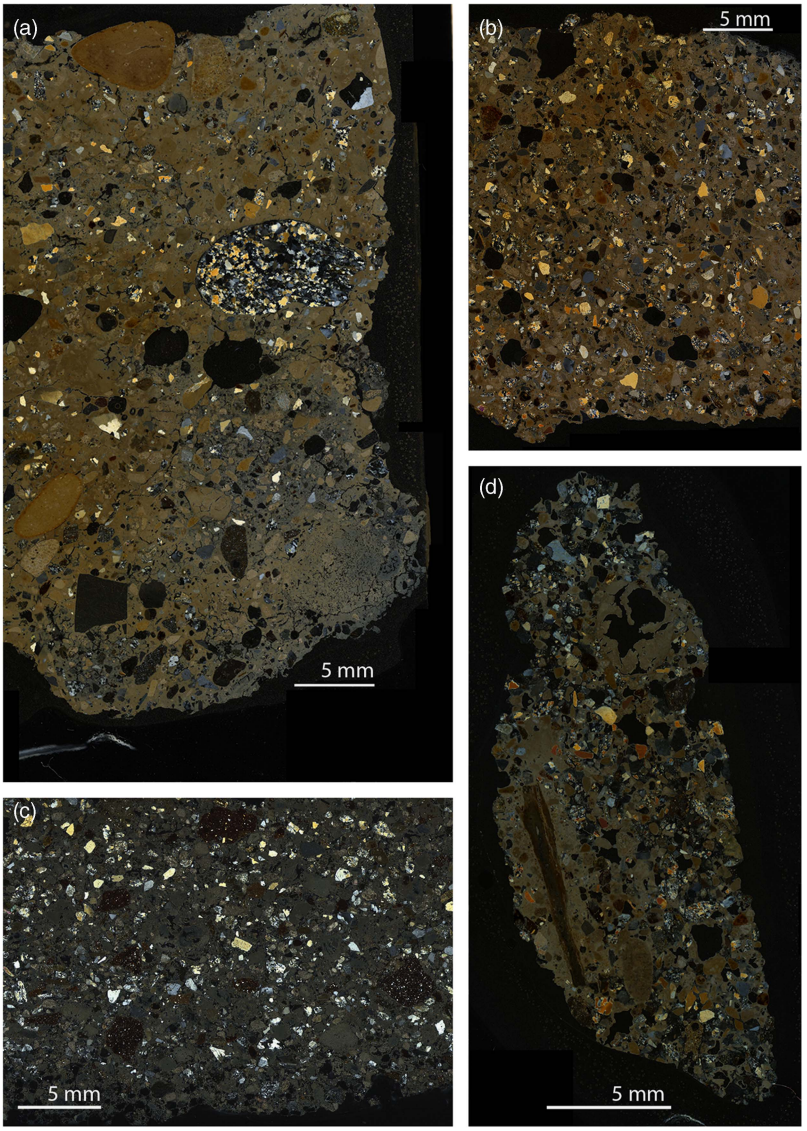

Figure 5 Transmitted light micrographs of mortar samples 276-36 (a), 201-39 (b), BP-M (c), and 202 (d).

with a weak red luminescence were observed. The estimated porosity is about 20% and no secondary calcite formed into the pore was observed. Charcoal residues of the fuel used for the combustion of the limestone were detected (Figure 7).

Mineralogically (Table 2), 276-36, 276-41, and BP-M samples have diffraction patterns characterized by a dominant carbonate composition (calcite and dolomite), high amount of silicate minerals (quartz and feldspars) and low amount of clays (illite and chlorite). As observed during the petrographic analysis, calcite is related both to the binder and the aggregate fraction, which is also composed by dolomite, quartz and feldspars. A few percentages of clay minerals (illite

https://doi.org/10.1017/RDC.2018.147 Published online by Cambridge University Press

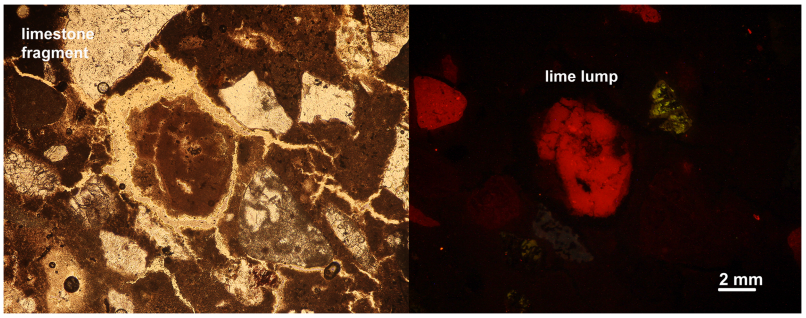

Figure 6 Mortar sample 276-36 in optical transmitted light (left) and in cathodoluminescence optical spectroscopy (right).

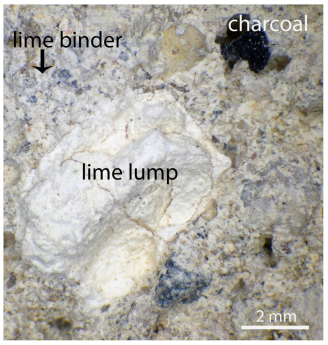

Figure 7 Binder, lime lump, and charcoal in sample BP-M.

and chlorite) and an amorphous fraction were detected as results of the occurrence of a soil fraction accidentally added to the lime mixture.

Based on the mortar characterization, three types of potentially datable materials were identified, i.e. the lime binders, the lime lumps and charcoal residues, the latter in mortar BP-M. This analysis reveals the risk of dead carbon contaminations due to the occurrence of small-grained carbonate aggregates in the binder and not-calcined fragments of limestone in the lumps. In samples 276, red luminescent lime lumps—that could be attributable to limestone residues— could heavily bias the ^{14}C signal of the binder if not removed through the purification treatment. On the other hand, the binder matrix does not shown luminescence indicating an aerial lime binder. In sample BP-M, the small-grained carbonate aggregates are unfortunately hardly separable from the binder through the gravimetric separation step of the purification treatment. Such a problem has also been encountered in the Medieval mortar mixer from Basel Cathedral Hill (Switzerland) selected for the MODIS round-robin exercise (Hajdas et al. 2017; Hayen et al 2017).

US 201 (Building III)

The mortar binders of US 201 (mortar 201-33 and 201-39—Figure 5b—sampled in two different points of the stratigraphic unit 201) are calcium lime binders with micritic textures. The amount of lime lumps is high, especially in sample 201-33, indicating an inappropriate

https://doi.org/10.1017/RDC.2018.147 Published online by Cambridge University Press

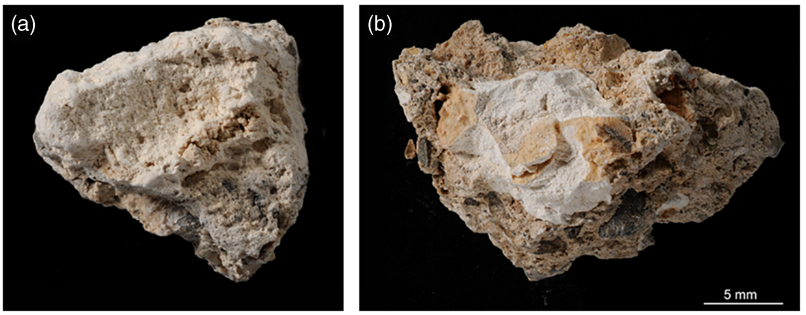

Figure 8 Lime lumps in samples 201-39 (a) and 201-33 (b).

Table 2 Mineralogical quantitative phase analysis (in wt %) of the mortar samples. Estimated errors are in the range 0.5–1.0 wt % for the mineralogical phases, and about 3–5 wt % for the amorphous phase. nd = not detected.

Sample	Amorphous C.	Calcite	Dolomite	Quartz	Feldspar	Micas	Illite	Clinochlore	Hydrotalcite
BP-M	4.8	33.9	16.1	18.9	16.8	2.0	4.5	3.0	nd
276-36	3.5	38.0	16.6	22.1	13.3	2.4	nd	4.0	nd
276-41	7.2	46.4	12.7	18.5	11.2	1.2	nd	2.7	nd
201-33	14.8	46.6	1.0	10.0	12.1	1.8	3.3	5.6	4.8
201-39	12.8	53.5	9.7	7.2	8.8	0.3	4.1	3.7	nd
202	11.1	21.2	16.2	30.3	17.1	0.8	nd	3.2	nd

mixing technology. As suggested by their friable and porous texture, the lime lumps of sample 201-33 were formed by a partial carbonation of the lime putty (Figure 8a). The presence of incompletely calcined limestone residues in some of the lumps are observed by red cathodo-luminescence. On the other hand, several lime lumps in sample 201-39 (Figure 8b) do not show cathodo-luminescence signal, so that they are potentially suitable for dating even if their compact texture might imply some degree of delayed carbonation.

The fine grained aggregate (0.04–0.90 mm) is mainly composed by quartzite, monocrystalline quartz, plagioclase feldspars and fragments of carbonate rocks (Table 1).

Mineralogically (Table 2), samples 201-33 and 201-39 differ from the mortars of the Roman structures (US 276 and BP-M) due to the occurrence of higher amounts of calcite and amorphous content, and lower percentages of silicate fraction. In sample 201-33, hydrotalcite–a mineral of the family of double-layered mixed-metal hydroxides (LDH or AFm in the cement systems)–was detected through x-ray powder diffraction. The presence of hydrotalcite indicates that localized pozzolanic reactions (Secco et al. 2016) occurred in the mortars of US-201 due to hydraulic components. The minero-petrographic characterization of sample US 201 indicates that the binders and the lime lumps could potentially be used for dating. However, the analysis reveals the risk of two types of contaminations: (1) dead carbon contaminations from either the carbonate aggregate in the binder or uncalcined limestone particles in the lime lumps, and (2) younger ^{14}C contamination from both LDH phases and delayed lime lump reaction.

https://doi.org/10.1017/RDC.2018.147 Published online by Cambridge University Press

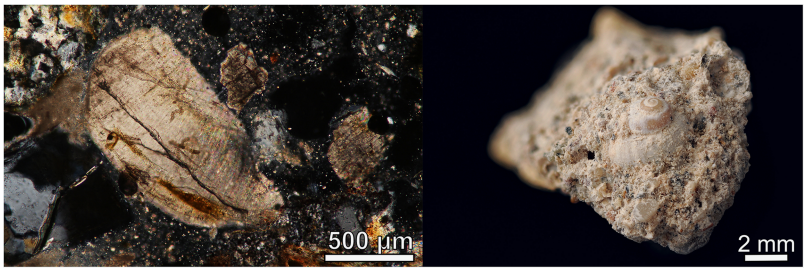

Figure 9 Shell fragment in mortar 202 observed in cross-polarized light (left) and under a stereomicroscope (right).

US 202 (Building IV)

Sample 202 (Figure 5d) is a lean mortar characterized by a brown mass color. The binder presents a homogenous aspect that means absence of impurities and presence of micritic texture, indicating an air hardening lime mortar. Different typologies of lime lumps were observed, due both to agglomeration of lime related to limited homogeneity during the mixing (weak cathodo-luminescence), and under-burned limestone fragments (high red cathodo-luminescence). The aggregate fraction presents a maximum and minimum diameter of about 1.3 and 0.03 mm, respectively. It is composed by quartzite, micritic and microsparitic carbonate lithoclasts, K-feldspar and it incorporates a few fresh water shell fragments (Figure 9). Several charcoal residues were also observed and sampled.

As suggested by the petrographic analysis, sample 202 is characterized by a highly dominant silicate fraction formed by quartz (30% wt) and feldspars (17% wt), that are related to the aggregate used. The low amount of calcite (21% wt) confirms the lean nature of the mortar. A high amount of geologic dolomite was detected, consistent with the petrographic observations: this might represent a problem for dating if not carefully removed from the binder fraction. The high amorphous fraction detected is related to the occurrence of paracrystalline clays mixed with the binding material. The absence of LDH-type phases attested the lack of significant hydraulic reactions between the different components of the binding mortar.

The purified binder was selected for ^{14}C dating, because the mineralogical analysis by XRPD indicated no dolomite present. The shell fragments and charcoal particles represent potentially datable materials to compare with the results obtained on the binder.

^{14}C Dating of Binders, Charcoal, and Shell Fragments

All the mortar samples were treated by using the Cryo2Sonic v.2.0. In order to check the improvements of the purification protocol, in some mortars the first version of the Cryo2Sonic was used. Due to the low amount of the available materials, only in few cases the two methods were applied on the same sample. Moreover, ^{14}C dating was also performed as a cross-check on all other datable materials present into the mortars and selected during the first macroscopic characterization, such as the lime lumps, the charcoal residues, and the shell fragments.

Regarding the mortars of the first structures, BP-M was treated by Cryo2Sonic v2.0, 276-36 mortar was treated by using both the two methods and 276-41 mortar was purified by using the first version of the Cryo2Sonic.

https://doi.org/10.1017/RDC.2018.147 Published online by Cambridge University Press

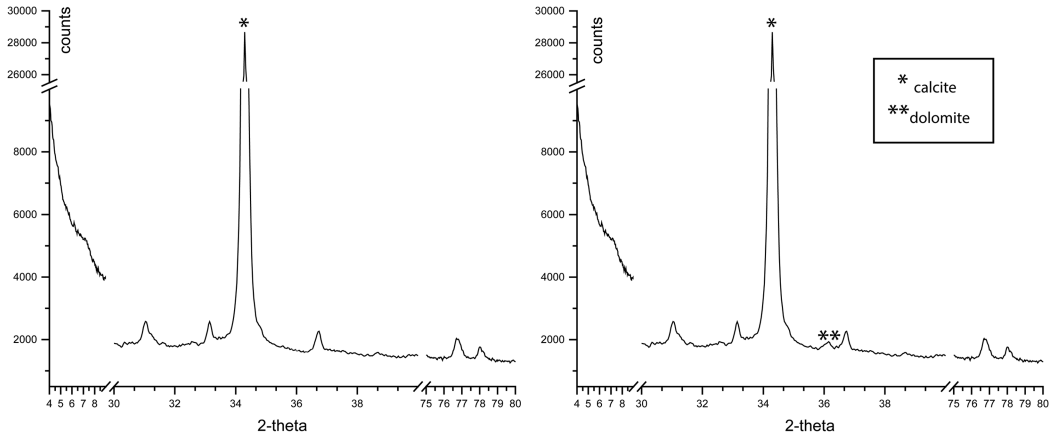

Figure 10 X-ray powder diffraction of the binder fraction of the 276-36 mortar treated by Cryo2Sonic v.2.0 (left). X-ray powder diffraction of the binder fraction of the 276-36 mortar treated by Cryo2Sonic, in which geogenic dolomite is detected (right).

The characterization of the purified powders after the treatments indicated the following:

1. The powder obtained from mortar 276-36 treated by Cryo2Sonic v.2.0 is devoid of geogenic carbonates (absence of red luminescence and dolomite), suggesting a good reliability for ^{14}C dating (Figure 10, left: 276-36 treated by Cryo2Sonic v.2.0). On the other hand, the powders obtained on the same mortar and on mortar 276-41 using the first version of Cryo2Sonic are contaminated by a high amount of geogenic carbonates observed under the cathodoluminescence microscope as red highly luminescent particles and indicated in XRPD analysis by the presence of geogenic dolomite (Figure 10, right: 276-36 treated by Cryo2Sonic).
2. The powders obtained from mortars BP-M treated by Cryo2Sonic v.2.0 still contain low amount of geogenic carbonates.
   The ^{14}C dates (Table 3) confirmed what was predicted by the check analyses: (1) 276-36 sample treated by Cryo2Sonic v2.0 presents a reliable ^{14}C date (219–380 AD, 2σ), matching the stylistic dating proposed for the Roman mosaic, and (2) the contaminated powders of mortars BP-M, 276-41 (Cryo2Sonic v2.0), and 276-36 (Cryo2Sonic) produced ^{14}C dating significantly older with respect to the ^{14}C age of the reliable binder powder. In order to verify the reliability of the ^{14}C charcoal dating, two charcoal residues collected from the mortar BP-M were dated. The ages obtained are (1) 236–379 AD (2σ) that are consistent with the one obtained by the powder extracted from 276-36 mortar through the Cryo2Sonic v.2.0; and (2) 34–214 AD, interpreted as a charcoal fragment likely affected by the *old wood* problem (Schiffer 1986; Regev et al. 2011). Regarding the lime lumps, for which the analysis indicated dead carbon contaminations, the samples collected from mortars BP-M and 276-36 were ^{14}C dated back to 126–252 AD and 3089–2884 BC, respectively. As predicted, the ^{14}C ages obtained from the lime lumps are older than expected.

Regarding the second structure, the mortar 201-39 was treated by both Cryo2Sonic v2.0 and Cryo2sonic, while mortar 201-33 was treated by the Cryo2Sonic method. The mortar powder 201-33 obtained by Cryo2Sonic is composed by calcite and low amount of hydrotalcite that

https://doi.org/10.1017/RDC.2018.147 Published online by Cambridge University Press

https://doi.org/10.1017/RDC.2018.147 Published online by Cambridge University Press

Table 3 Radiocarbon age determinations of the mortars of the Padua Cathedral. AAA: acid-alkali-acid treatment; XRPD: x-ray powder diffraction; CL: presence of luminescence; cc: calcite; dol: dolomite; hyt: hydrotalcite

US	Sample	Material	Treatment	XRPD	CL	RA yr BP ± 1σ	Cal. AD/BC age ranges (2σ)	Reliable RA
MOSAIC	BP-M	Charcoal	AAA	—	—	1746 ± 23	AD 236–AD 354 (97.3%) AD 367–AD 379 (2.7%)	Yes
	BP-M	Charcoal	AAA	—	—	1896 ± 30	AD 34–AD 35 (0.2%) AD 52–AD 214 (99.8%)	No
	BP-M	Purified binder	Cryo2Sonic v.2.0	cc, dol	Yes	1908 ± 28	AD 23–AD 143 (96.7%) AD 152–AD 169 (1.7%) AD 194–AD 208 (1.6%)	No
	BP-M	Lime lump	—	cc	Yes	1823 ± 26	AD 126–AD 252 (99.0%) AD 304–AD 312 (1.0%)	No
276	276-36	Purified binder	Cryo2Sonic v.2.0	cc	nd	1757 ± 27	AD 219–AD 359 (97.4%) AD 363–AD 380 (2.6%)	Yes
	276-36	Purified binder	Cryo2Sonic	cc, dol	Yes	2057 ± 29	BC 167–AD 3 (100%)	No
	276-36	Lime lump	—	cc, dol	Yes	4332 ± 47	BC 3089–BC 3052 (7.6%) BC 3033–BC 2884 (92.4%)	No
	276-41	Purified binder	Cryo2Sonic	cc, dol	Yes	2319 ± 49	BC 537–BC 349 (76.8%) BC 314–BC 208 (23.2%)	No
201	201-33	Purified binder	Cryo2Sonic	cc, hyt	nd	882 ± 36	AD 1038–AD 1223 (100%)	Doubt
	201-39	Purified binder	Cryo2Sonic v.2.0	cc	nd	987 ± 25	AD 993–AD 1051 (63%) AD 1082–AD 1128 (29.4%) AD 1135–AD 1151 (7.6%)	Yes
	201-39	Purified binder	Cryo2Sonic	cc	Yes	1310 ± 28	AD 657–AD 725 (72%) AD 738–AD 768 (28%)	No
	201-33	Lime lump	—	cc, dol	Yes	2378 ± 30	BC 722–BC 721 (0.2%) BC 703–BC 695 (0.8%) BC 541–BC 392 (99.0%)	No

https://doi.org/10.1017/RDC.2018.147 Published online by Cambridge University Press

	201-39	Lime lump	—	cc	nd	688 ± 38	AD 1261–AD 1321 (65.7%) AD 1348–AD 1392 (34.3%)	Doubt
202	202	Purified binder	Cryo2Sonic v.2.0	cc	nd	1571 ± 29	AD 417–AD 551 (100%)	No
	202	Purified binder	Cryo2Sonic	cc	Yes	1475 ± 42	AD 433–AD 457 (3.2%) AD 468–AD 488 (3.2%) AD 533–AD 653 (93.6%)	No
	202	Charcoal	AAA	—	—	1012 ± 31	AD 971–AD 1049 (87.2%) AD 1085–AD 1124 (10.3%) AD 1137–AD 1150 (2.5%)	Yes
	202	Shell	H_3PO_4	—	—	1522 ± 26	AD 429–AD 494 (31%) AD 508–AD 519 (1.9%) AD 528–AD 604 (67.1%)	No

contaminated the sample giving younger ^{14}C age (Table 3). On the other hand, the sample 201-39 purified by Cryo2Sonic is characterized by the presence of geological carbonate and its ^{14}C dating is heavily affected by this contaminant. The same mortar (201-39) treated by Cryo2-Sonic v.2.0 is characterized by the absence of geogenic dolomite and it shows a clean cathodoluminescence and x-ray powder diffraction profiles. The check analysis indicated that 201-39 (Cryo2Sonic v.2.0) is the unique reliable sample for ^{14}C dating and the date obtained confirmed this, being in accordance with the archaeological evidence (10th century AD). The lime lumps sampled from 201–33 (high luminescence) and 201–39 (non-luminescent) mortars were ^{14}C dated to 722–392 BC and AD 1261–1392, respectively. As expected from the preliminary characterization, the 201-33 lime lump was clearly contaminated by geological carbonate, having an over burnt limestone core that affected the ^{14}C age determination. On the contrary, the 201-39 lime lump was likely suffering from poor reactivity due to an insufficient slaking process. Therefore, this lime lump hardened well after the binder, generating a younger ^{14}C signal.

The mortar of sample US 202 was treated by using both methods and the obtained powders are apparently devoid of geological carbon—in fact, no red luminescence or dolomite was detected. However, both ^{14}C dating performed indicated ages between 5th and 7th centuries AD, not compatible with the archaeological evidence. The incongruence is thought to be caused by the diffuse presence of fine shell fragments that were ^{14}C dated to 429–653 AD, after a careful cleaning in ultra-pure water (by Goslar at al. 2009). Therefore, the binder is severely affected by a freshwater shell contribution, which cannot be physically separated at the moment and it is undetected by cathodo-luminescence spectroscopy. Dating of the charcoal residues sampled on the mortar yield a ^{14}C age of 971–1150 AD with the highest probability interval of 971–1049 AD (87.2%, 2σ), in agreement with the archaeological evidence.

DISCUSSION AND CONCLUSION

This research is an example of a multi-disciplinary study encompassing the successful interaction between materials scientists and archaeologists, which greatly helped in placing the measured materials into appropriate archaeological and stratigraphic context. The identification of different ancient structures excavated next to the Romanesque baptistery of Padua and their ^{14}C dating reported here allow the location and dating of the first episcopal complex of Padua.

The architectural structures were radiocarbon dated by measuring the ^{14}C of the materials contained in the structural mortars: the calcite fraction of binders, the lime lumps, the charcoal residues, and some shell fragments. The mortar samples were treated following the optimized Cryo2Sonic v.2.0 protocol and its original version.

The ^{14}C dates indicate that the oldest structure is Building II, where the mortar (US 276) was dated to 3rd–4th centuries AD by using the Cryo2Sonic v.2.0. Consistent ^{14}C age determinations were obtained between the charcoal fragment sampled from the binder of the Roman mosaic mortar (BP-M) and the binder fraction of the surrounding wall (276-36 and 276-41). These ^{14}C ages give the oldest absolute ^{14}C ages of excavated structures suggesting that this was the first religious complex of Padua in accordance with the first mention of a Padua bishop, Crispino in 343 AD (Chavarría 2017).

Building III (US 201) and Building IV (US 202) are related to a later period. Building III was dated to the 10th century AD by measuring the ultra-pure binder fraction that was obtained by using the Cryo2Sonic v.2.0 (sample 201-39), while Building IV was dated by measuring the

https://doi.org/10.1017/RDC.2018.147 Published online by Cambridge University Press

charcoal fragments contained into the mortar matrices (sample 202). In fact, it is shown that a substantial amount of fine-grained fresh water shell contaminated the binder of mortar 202; ^{14}C ages are consequently biased from the calcitic content of shell fragments, which were independently dated and found to be older that the age of the structure. Based on the age obtained on the binder and charcoal fragments, the Building III and Building IV are coeval.

Regarding the evolution of the binder treatment, the current state of the research indicates the following:

1. The proposed Cryo2Sonic v. 2.0 protocol considerably improved the degree of the binder purification efficiency. In fact, the gravimetric sedimentation step allowed us to obtain a complete separation of the calcium carbonate binder particles from the other components of the mortars in several cases, such as the geogenic carbonate aggregate. This was verified in the case of the mortars sampled from US 276 and US 201 contaminated by a carbonate sand, for which the original Cryo2Sonic method systematically provided ages older than expected. The usage of version 2.0 of the method provided highly purified samples, leading to reliable ^{14}C ages;
2. In order to date mortar, the most reliable material is the purified binder, for which the potential for dating can be verified *a priori*. In the present study, the lime lumps are shown to be significantly affected by contaminations shifting the measured ^{14}C ages to older or even younger dates. The ^{14}C dating of charcoal residues is usually reliable and, if present, it can be used to date the architectural structure. However, caution should be exerted, since as observed in mosaic mortar BP-M, the ^{14}C ages of two charcoal residues extracted from the same mortar could produce conflicting results, likely due to the *old wood problem*. Further, even shell fragments—usually problematic materials inside the mortars since their ^{14}C content can differ from the atmosphere depending on the formation habitat (i.e. sea, lake, river, land)—resulted in unreliable dates, caused by older re-worked shell material.

The results of the present investigation clearly indicate that mortar materials need to be carefully characterized before undergoing ^{14}C dating. It is proposed that a full characterization of the mortars and the binder fractions may lead to (1) a better assessment of the nature of the mortar components and their contexts, (2) an indication of the proper materials to be ^{14}C dated or avoided, and (3) a more informed protocol for the whole dating process.

Several residual problems in the process need to be investigated and hopefully resolved in the future. The most important ones, as also evidenced in the course of the recent MODIS round-robin (Hajdas et al. 2017; Hayen et al 2017) are (1) the detection and the elimination of the contamination derived from CO_3^{2-}-bearing LDH phases present in the lime mortars affected by hydraulic reactions, and (2) the effective separation of the datable binder fraction from the ultra-fine fraction of geologic carbonate that at present cannot be eliminated by either physical or chemical methods.

ACKNOWLEDGMENTS

The excavation and study of the remains were funded by the Fondazione Cassa di Risparmio di Padova e Rovigo. We are grateful to Aurelio Giaretta (Consiglio Nazionale delle Ricerche – Istituto di Geoscienze e Georisorse) for his help during experimentation, and Stefano Castelli, Leonardo Tauro and Federico Zorzi of the University of Padua – Department of Geosciences for their help for sample preparation. Two anonymous reviewers and Associate Editor Hans van der Plicht are acknowledged for insightful comments on a preliminary version of the manuscript.

https://doi.org/10.1017/RDC.2018.147 Published online by Cambridge University Press

REFERENCES

Artioli G, Secco M, Addis A, Bellotto M. 2017. Role of hydrotalcite-type layered double hydroxides in delayed pozzolanic reactions and their bearing on mortar dating. In: Pöllmann H, editor. Cementitious materials. Composition, properties, application. De Gruyter: in press.

Canci A, Marinato M, Zago M. 2017. Le aree cimiteriali: studio bioarcheologico. In: Chavarría Arnau, editor. Ricerche sul centro episcopale di Padova. Scavi 2011-2012, Mantova, SAP s.r.l.: 131–150.

Chavarría Arnau A. 2017. La cristianizzazione di Padova e le origini del complesso episcopale. In: Chavarría Arnau A, editor. Ricerche sul centro episcopale di Padova. Scavi 2011–2012, Mantova, SAP s.r.l.: 367–372.

Goslar T, Nawrocka D, Czernik J. 2009. Foraminiferous limestone in ^{14}C dating of mortar. Radiocarbon 51(3):987–993.

Hajdas I, Lindroos A, Heinemeier J, Ringbom Å, Marzaioli F., Terrasi F, Passariello I, Capano M, Artioli G, Addis A, Secco M, Michalska D, Czernik J, Goslar T, Hayen R, Van Strydonck M, Fontaine L, Boudin M, Maspero F, Panzeri L, Galli A, Urbanova P, Guibert P. 2017. Preparation and dating of mortar samples. Mortar Dating Inter-comparison Study (MODIS). Radiocarbon 59(6):1845–1858.

Hayen R, Van Strydonck M, Fontaine L, Boudin M, Lindroos A, Heinemeier J, Ringbom Å, Michalska D, Hajdas I, Hueglin S, Marzaioli F, Terrasi F, Passariello I, Capano M, Maspero F, Panzeri L, Galli A, Artioli G, Addis A, Secco M, Boaretto E, Moreau C, Guibert P, Urbanova P, Czernik J, Goslar T, Caroselli M. 2017. Mortar dating methodology: Intercomparison of available methods. Radiocarbon 59(6):1859–1871.

Heinemeier J, Ringbom Å, Lindroos A, Sveinbjörnsdóttir ÁE. 2010. Successful AMS ^{14}C dating of non-hydraulic lime mortars from the Medieval churches of the Åland Islands, Finland. Radiocarbon 52(1):171–204.

Lindroos A, Heinemeier J, Ringbom Å, Braskén M, Sveinbjörnsdóttir Á. 2007. Mortar dating using AMS ^{14}C and sequential dissolution: examples from Medieval, non-hydraulic lime mortars from the Åland Islands, SW Finland. Radiocarbon 49 (1):47–67.

Marzaioli F, Borriello G, Passariello I, Lubritto C, De Cesare N, D'Onofrio A, Terrasi F. 2008. Zinc reduction as an alternative method for AMS radiocarbon dating: Process optimization at CIRCE. Radiocarbon 50 (1):139–149.

Marzaioli F, Lubritto C, Nonni S, Passariello I, Capano M, Terrasi F. 2011. Mortar radiocarbon dating: preliminary accuracy evaluation of a novel methodology. Analytical Chemistry 83:2038–2045.

Marzaioli F, Nonni S, Passariello I, Capano M, Ricci P, Lubritto C, De Cesare N, Eramo G, Castillo IAQ, Terrasi F. 2013, Accelerator mass spectrometry ^{14}C dating of lime mortars: Methodological aspects and field study applications at CIRCE (Italy). NIMB 294:246–251.

Michalska D, Pazdur A, Czernik J, Szczepaniak M, Zurakowska M. 2013. Cretaceous aggregate and reservoir effect in dating the binding materials. Geochronometria 40:33–41.

Michalska D, Czernik J. 2015. Carbonates in leaching reactions in context of ^{14}C dating. Nuclear Instruments and Methods in Physics Research B 361:431–439.

Nawrocka D, Michniewicz J, Pawlyta A. 2005. Application of radiocarbon method for dating of lime mortars. Journal on Methods and Applications of Absolute Chronology, GEOCHRONOMETRIA 24:109–115.

Nawrocka D, Czernik J, Goslar T. 2009. ^{14}C dating of carbonate mortars from Polish and Israeli sites. Radiocarbon 51(2):857–866.

Nonni S, Marzaioli F, Secco M, Passariello I, Capano M, Lubritto C, Mignardi S, Tonghini S, Terrasi F. 2013. ^{14}C mortar dating: The case of the medieval Shayzar Citadel, Syria. Radiocarbon 55(2):514–525.

Passariello I, Marzaioli F, Lubritto C, Rubino M, d'Onofrio A, de Cesare N, Borriello G, Casa G, Palmieri A, Rogalla D, Sabbarese C, Terrasi F. 2007. Radiocarbon sample preparation at the CIRCE AMS laboratory in Caserta, Italy. Radiocarbon 49(2):225–232.

Ramsey CB, Lee S. 2013. Recent and planned developments of the program OxCal. Radiocarbon 55 (2):720–730.

Regev L, Eckmeier E, Mintz E, Weiner S, Boaretto E. 2011. Radiocarbon concentrations of wood ash calcite: potential for dating. Radiocarbon 53 (1):117–127.

Reimer PJ, Bard E, Bayliss A, Beck JW, Blackwell PG, Bronk C, Ramsey, Grootes PM, Guilderson TP, Haflidason H., Hajdas J., Hattž C, Heaton TJ, Hoffmann DI, Hogg AG, Hughen KA, Kaiser KF, Kromer B, Manning SW, Niu M, Reimer RW, Richards DA, Scott EM, Southon JR, Staff RA, Turney CSM, van der Plicht J. 2013, IntCal13 and Marine13 radiocarbon age calibration curves 0–50,000 years cal BP. Radiocarbon 55(4):1869–1887.

Rietveld H. 1969. A profile refinement method for nuclear and magnetic structures. Journal of Applied Crystallography 2:65–71.

Rozansky K, Stichler W, Gonfiantini R, Kromer B, van der Plicht J. 2002. The IAEA ^{14}C intercomparison exercise 1990. Radiocarbon 34 (3):506–519.

Schiffer MB. 1986. Radiocarbon dating and the "old wood" problem: the case of the Hohokam chronology. Journal of Archaeological Science 13(1):13–30.

https://doi.org/10.1017/RDC.2018.147 Published online by Cambridge University Press

Secco M, Addis A, Artioli G. 2016. Characterization of lime-stabilized earthen mortars from historic masonry structures. In Modena C, da Porto F, Valluzzi MR, editors. Proceedings of IB2MAC 2016 – 16th International Brick and Block Masonry Conference, Padova, 26–30 June 2016. CRC Press/Balkema. p. 1889–1896.

Sonninen E, Jungner H. 2001. An improvement in preparation of mortar for radiocarbon dating. Radiocarbon 43(2A):271–273.

Terrasi F, Rogalla D, De Cesare N, D'Onofrio A, Lubritto C, Marzaioli F, Passariello I, Rubino M, Sabbarese C, Casa G, Palmieri A, Gialanella I, Imbriani G, Roca V, Romano M, Sundquist M, Loger R. 2007. A new AMS facility in Caserta/Italy. Nuclear Instruments and Methods in Physics Research B 259:14–17.

Terrasi F, De Cesare N, D'Onofrio A, Lubritto C, Marzaioli F, Passariello I, Rogalla D, Sabbarese C, Borriello G, Casa G, Palmieri A. 2008. High precision ^{14}C AMS at CIRCE. Nuclear Instruments and Methods in Physics Research B 266:2221–2224.

Van Strydonck M, Dupas M, Dauchot-Dehon M. 1983a. Radiocarbon dating of old mortars. In Mook WG and Waterbolk HR editors. ^{14}C and Archaeology Proceedings, PACT 8:337–343.

Van Strydonck M, Dupas M, Dauchot-Dehon M, Pachiaudi C, Marechal J. 1983b. A further step in the radiocarbon dating of old mortars. Bulletin Van Het Kon Inst. Voor het Kunstpatrimonium XIX:155–171.

Van Strydonck M, Dupas M. 1991. The classification and dating of lime mortars by chemical analysis and radiocarbon dating: A review. BAR International Series 574:5–43.

https://doi.org/10.1017/RDC.2018.147 Published online by Cambridge University Press